Markus Hautakorpi, Maija Mattinen, and Hanne Ludvigsen. 2008. Surface-plasmon-resonance sensor based on three-hole microstructured optical fiber. Optics Express, volume 16, number 12, pages 8427-8432.

Surface-plasmon-resonance sensor based on three-hole microstructured optical fiber

Markus Hautakorpi, Maija Mattinen, and Hanne Ludvigsen

Fiber Optics Group, Department of Micro and Nanosciences, Helsinki University of Technology, P.O.Box 3500, FI-02015 TKK, Finland

markus.hautakorpi@tkk.fi

Abstract: We propose a novel surface-plasmon-resonance sensor design based on coating the holes of a three-hole microstructured optical fiber with a low-index dielectric layer on top of which a gold layer is deposited. The use of all three fiber holes and their relatively large size should facilitate the fabrication of the inclusions and the infiltration of the analyte. Our numerical results indicate that the optical loss of the Gaussian guided mode can be made very small by tuning the thickness of the dielectric layer and that the refractive-index resolution for aqueous analytes is 1×10^{-4}.

OCIS codes: (060.2280) Fiber design and fabrication; (060.2340) Fiber optics components; (240.6680) Surface plasmons.

References and links

1. P. J. A. Sazio, A. Amezcua-Correa, C. E. Finlayson, J. R. Hayes, T. J. Scheidemantel, N. F. Baril, B. R. Jackson, D.-J. Won, F. Zhang, E. R. Margine, V. Gopalan, V. H. Crespi, and J. V. Badding, "Microstructured optical fibers as high-pressure microfluidic reactors," Science **311,** 1583–1586 (2006).
2. X. Zhang, R. Wang, F. Cox, B. T. Kuhlmey, and M. C. J. Large, "Selective coating of holes in microstructured optical fiber and its application to in-fiber absorptive polarizers," Opt. Express **15,** 16270–16278 (2006).
3. A. Amezcua-Correa, J. Yang, C. E. Finlayson, A. C. Peacock, J. R. Hayes, P. J. A. Sazio, J. J. Baumberg, and S. M. Howdle, "Surface-enhanced Raman scattering using microstructured optical fiber substrates," Adv. Funct. Mater. **17,** 2024–2030 (2007).
4. B. T. Kuhlmey, K. Pathmanandavel, and R. C. McPhedran, "Multipole analysis of photonic crystal fibers with coated inclusions," Opt. Express **14,** 10851–10864 (2006).
5. A. Hassani and M. Skorobogatiy, "Design of the microstructured optical fiber-based surface plasmon resonance sensor with enhanced microfluidics," Opt. Express **14,** 11616–11621 (2006).
6. A. Hassani and M. Skorobogatiy, "Design criteria for microstructured-optical-fiber-based surface-plasmon-resonance sensors," J. Opt. Soc. Am. B **24,** 1423–1429 (2007).
7. B. Gauvreau, A. Hassani, M. F. Fehri, A. Kabashin, and M. Skorobogatiy, "Photonic bandgap fiber-based surface plasmon resonance sensors," Opt. Express **15,** 11413–11426 (2007).
8. Y. Ruan, E. P. Schartner, H. Ebendorff-Heidepriem, P. Hoffmann, and T. M. Monro, "Detection of quantum-dot labeled proteins using soft-glass microstructured optical fibers," Opt. Express **15,** 17819–17826 (2007).
9. S. Afshar V., S. C. Warren-Smith, and T. M. Monro, "Enhancement of fluorescence-based sensing using microstructured optical fibers," Opt. Express **15,** 17891–17901 (2007).
10. C. M. B. Cordeiro, M. A. R. Franco, C. J. S. Matos, F. Sircilli, V. A. Serrão, and C. H. Brito Cruz, "Single-design-parameter microstructured optical fiber for chromatic dispersion tailoring and evanescent field enhancement," Opt. Lett. **32,** 3324–3326 (2007).
11. M. C. P. Huy, G. Laffont, V. Dewynter, P. Ferdinand, P. Roy, J. -L. Auguste, D. Pagnoux, W. Blanc, and B. Dussardier, "Three-hole microstructured optical fiber for efficient fiber Bragg grating refractometer," Opt. Lett. **32,** 2390–2392 (2007).
12. http://www.comsol.com/
13. E. D. Palik, ed., *Handbook of Optical Constants of Solids* (Academic Press, San Diego, Calif., 1998).

#93743 - $15.00 USD Received 11 Mar 2008; revised 23 Apr 2008; accepted 16 May 2008; published 9 Jun 2008

14. H. P. Uranus, "A simple and intuitive procedure for evaluating mode degeneracy in photonic crystal fibers," Am. J. Phys. **74,** 211–217 (2006).
15. G. P. Agrawal, *Nonlinear Fiber Optics*, 3rd ed. (Academic Press, San Diego, Calif., 2001).
16. S. Kim, Y. Jung, K. Oh, J. Kobelke, K. Schuster, and J. Kirchhof, "Defect and lattice structure for air-silica index-guiding holey fibers," Opt. Lett. **31,** 164–166 (2006).

1. Introduction

Quite recently, Sazio *et al.* [1] demonstrated that high-pressure chemical deposition techniques can be used to uniformly coat the hole surfaces of a microstructured optical fiber (MOF) with a variety of materials, e.g., with gold. Later on, the excitation of plasmon resonances in MOFs with coated metal inclusions have actively been studied using both experimental [2, 3] and numerical [4, 5, 6, 7] methods. The resonance wavelength of the plasmon excitation strongly depends on the dielectric function of the material in contact with the metal. Owing to this characteristic, compact fiber-optic surface-plasmon-resonance (SPR) sensors for liquid substances can be constructed by infiltrating the analyte into the metal-coated holes of the MOF. The refractive index of the analyte can then be retrieved either by measuring the transmission spectrum or by monitoring the transmitted power at certain wavelength. So far, numerical analyses of such MOF-integrated SPR sensors based on both index-guiding [5, 6] and bandgap-guiding [7] fibers have been reported. In these proposed designs, however, selective coating and filling of the fiber holes are required.

In this paper, we propose a novel SPR sensor design based on coating the inner surfaces of a three-hole MOF with a dielectric layer on top of which a gold layer is deposited. The use of all three fiber holes along with their notably large size should facilitate the fabrication of the inclusions and the infiltration of the analyte. The low-index dielectric is sandwiched between the original MOF and a thin layer of gold to control the overlap between the fundamental core mode and the gold coating. We investigate numerically the excitation of plasmon resonances in the proposed sensor fiber. Three-hole MOFs, also termed suspended-core fibers, have previously been applied mainly in evanescent-wave sensing [8, 9] but also in dispersion management [10] and in the construction of a fiber Bragg grating refractometer [11].

This paper is organized as follows. In Section 2, we detail the proposed design and the numerical modeling procedure. The dependence of the plasmon-resonance loss spectrum on the essential design parameters is characterized in Section 3. The paper is summarized and concluded with a discussion in Section 4.

2. Sensor design and numerical modeling

We start by considering a three-hole MOF, such as the one shown in Fig. 1(a). For sensor operation, the hole surfaces are first uniformly coated with an auxiliary dielectric layer of thickness s. The layer is assumed to have a lower refractive index than that of the original MOF to provide mode confinement. Then, on top of this auxiliary layer, a gold layer of thickness d is deposited. The cross section of the resulting structure is schematically depicted in Fig. 1(b). The center of curvature dictating the core shape [point P in Fig. 1(b)] is taken to shape the coated layers as well [1]. Lastly, the fiber holes are assumed to be filled with an aqueous analyte.

The electromagnetic mode of the sensor fiber is solved with the finite element method (FEM) by using COMSOL Multiphysics software [12]. For the FEM modeling, we fix the radius of curvature to $r = 4\ \mu$m and the thickness of the core struts to $c = 200$ nm. The refractive indices of the original MOF and the low-index layer are chosen to roughly correspond to doped silica. For gold, we use the tabulated refractive-index values [13] with linear interpolation between the data points. To reduce the computation time, we assume that only the core and its struts are coated. Furthermore, only one half of the structure needs to be considered thanks to its

#93743 - $15.00 USD Received 11 Mar 2008; revised 23 Apr 2008; accepted 16 May 2008; published 9 Jun 2008

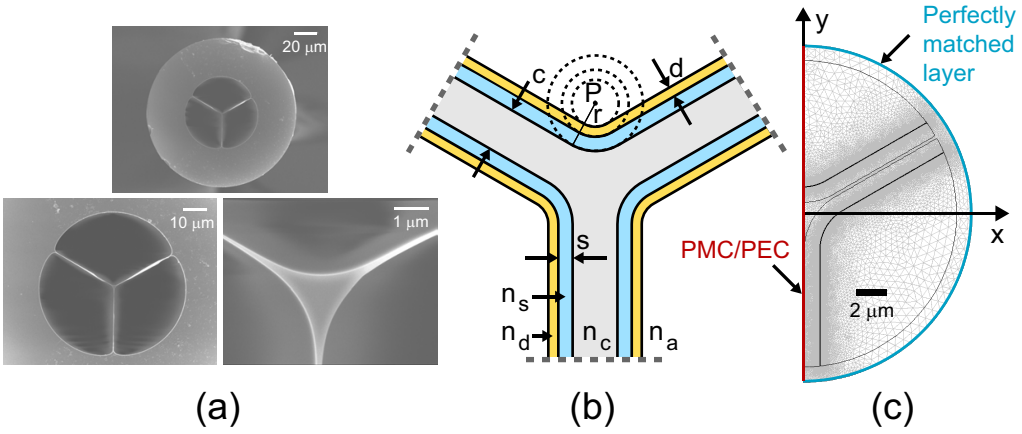

Fig. 1. (a) Cross-section images of a three-hole MOF fabricated at the University of Marie Curie-Sklodowska, Lublin, Poland (printed with permission). (b) Surroundings of the core in the proposed sensor fiber. Parameters s (n_s), c (n_c), and d (n_d) denote the thickness (refractive index) of the auxiliary dielectic layer, the core strut, and the gold layer, respectively. The background refractive index is that of the analyte, n_a, and r denotes the radius of curvature from point P. (c) Example FEM mesh and boundary conditions.

symmetry properties [14]. Halving of the structure gives rise to an artificial boundary which is taken to be either a perfect magnetic conductor (PMC) or a perfect electric conductor (PEC). The corresponding boundary conditions are written as $\mathbf{n}\times\mathbf{H}=\mathbf{0}$ and $\mathbf{n}\times\mathbf{E}=\mathbf{0}$, respectively, with $\mathbf{n}$ being a unit vector perpendicular to the boundary and $\mathbf{H}$ ($\mathbf{E}$) denoting the magnetic (electric) field. At the remaining outer border, a perfectly matched layer is chosen to handle the boundary condition. Figure 1(c) shows an example FEM mesh along with the boundary conditions at the borders of the computing region. Within the computing region, continuity of the tangential field components across the material boundaries is assumed.

In order to find the propagating mode of the sensor, we solve the vector wave equation

$$\nabla\times\varepsilon^{-1}\nabla\times\mathbf{H}=k_0^2\mathbf{H} \tag{1}$$

with the following ansatz

$$\mathbf{H}(x,y,z;t)=\mathbf{H}(x,y)e^{-i(\beta z-\omega t)}. \tag{2}$$

Here, ε describes the relative, complex dielectric function, $k_0=2\pi/\lambda$ is the wavenumber with λ being the free-space wavelength, ω is the angular frequency of light, and t denotes time. The propagation constant can be expressed as

$$\beta=n_{\text{eff}}k_0, \tag{3}$$

where n_{eff} is the effective index of the mode. The decay in the power of the mode as it propagates through the sensor fiber (toward the positive z direction) can be described with the formula

$$P=P_0e^{-\alpha z}, \tag{4}$$

where P_0 is the power at the plane $z=0$. The attenuation constant α is proportional to the imaginary part of the effective index according to the relation

$$\alpha=2k_0\text{Im}(n_{\text{eff}}). \tag{5}$$

#93743 - $15.00 USD Received 11 Mar 2008; revised 23 Apr 2008; accepted 16 May 2008; published 9 Jun 2008

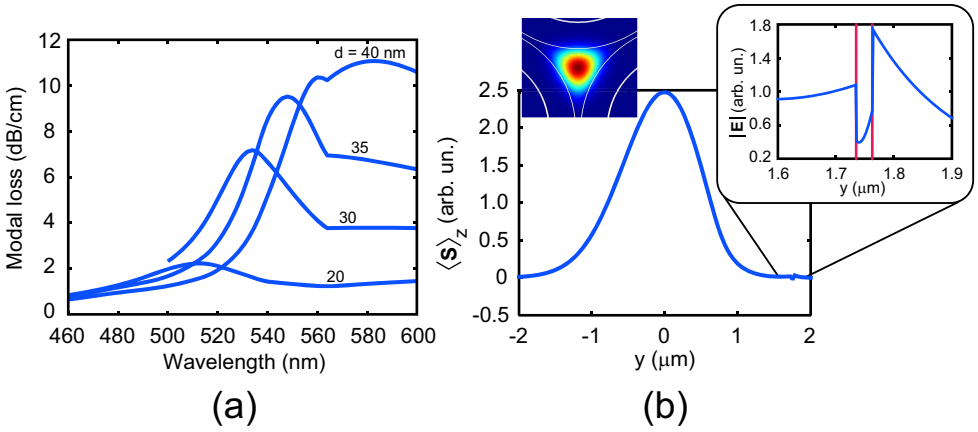

Fig. 2. (a) Modal loss α as a function of wavelength for different gold layer thicknesses d. (b) Longitudinal component of the time-averaged Poynting vector, $\langle \mathbf{S} \rangle_z$, on the y-axis. Left inset: cross-sectional view of the mode profile. Right inset: close-up of the norm of the electric field with the vertical lines marking the gold layer location.

We use the parameter α to quantify the propagation loss of the Gaussian guided modes which are obtained by using either the PMC or the PEC boundary conditions. These modes are degenerate within the accuracy of our computations.

3. Results

The modal propagation loss peaks at the plasmon-resonance wavelength which depends not only on the analyte but also on the thickness of the gold layer. Figure 2(a) shows the modal loss as a function of wavelength for different thicknesses of the gold layer. The thickness of the dielectric layer is fixed to $s = 1.5$ μm and the refractive indices of the original MOF, the dielectric layer, and the analyte are taken to be $n_c = 1.46$, $n_s = 1.44$, and $n_a = 1.33$, respectively. The sharp bends in the curves near $\lambda = 564$ nm originate from the use of the tabulated refractive-index data for gold. Consequently, we fix the gold layer thickness to $d = 30$ nm in our further calculations to clearly distinguish the plasmon resonance. Figure 2(b) illustrates the spatial characteristics of the mode (here $s = 1$ μm and $\lambda = 530$ nm). The mode is very close to Gaussian in its overall shape throughout the loss peak. At the interface between the gold and the analyte, however, the field amplitude locally decays in both of the materials, which is a characteristic of plasmon excitation.

The plasmon amplitude and thus the overall loss of the sensor can be tuned to a tolerable level by selecting the layer thickness s appropriately. This is exemplified in Fig. 3(a) which shows the modal loss spectrum for several values of the parameter s. Two values, $n_a = 1.33$ and $n_a = 1.34$, are used for the refractive index of the analyte to assess the refractive-index resolution. The other refractive indices are taken to be $n_c = 1.46$ and $n_s = 1.44$. The peak wavelength and the analyte-dependent shift in the resonance peak, $\Delta\lambda_{\text{peak}}$, are identical for all values of s. Thus, the thickness-parameter s lends itself well to exclusively controlling the overall loss.

On the other hand, if the refractive index of the core is varied, as in Fig. 3(b), both the peak wavelength and the analyte-dependent shift $\Delta\lambda_{\text{peak}}$ will change. Here, we have fixed the parameters $s = 1.5$ μm and $n_s = 1.44$. The peak shift is at its strongest when the parameter n_c is in value close to n_s. In such a case, the small refractive-index contrast between the core and

#93743 - $15.00 USD Received 11 Mar 2008; revised 23 Apr 2008; accepted 16 May 2008; published 9 Jun 2008

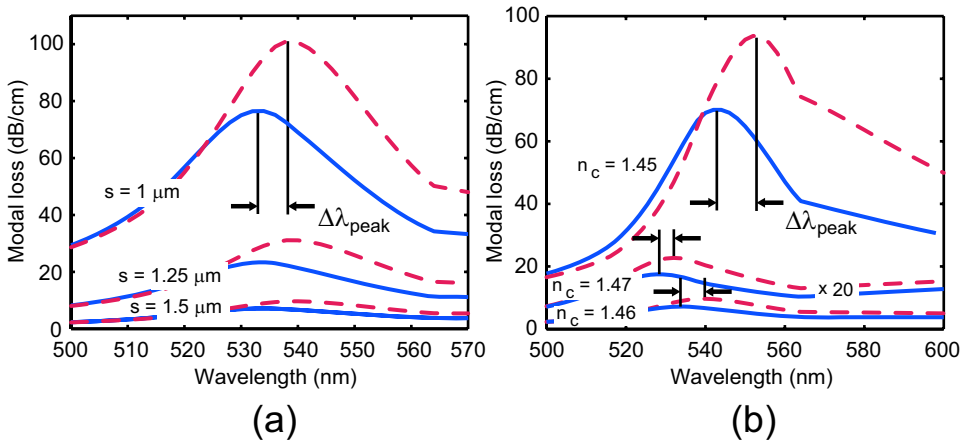

Fig. 3. Modal loss as a function of wavelength for two analytes with refractive indices $n_a = 1.33$ (solid) and $n_a = 1.34$ (dashed). The curves are plotted for (a) different dielectric layer thicknesses s and (b) different refractive indices n_c of the core. In (b), the data for $n_c = 1.47$ are magnified by a factor of 20 for clarity.

the auxiliary dielectric limits the number of core-confined modes. In particular, by choosing a small-core MOF to begin with, the device can be made to support a single transverse mode throughout the resonance peak. To estimate the required core dimension, we crudely approximate our sensor waveguide with a conventional step-index fiber that has an index contrast equal to $\Delta n = n_c - n_s = 0.01$. In such a case, the effective core radius, calculated through the V parameter [15], would have to be smaller than 1.1 μm. The dimensions in our design [see Fig. 1(c)] are on this order.

By measuring the transmission spectrum of the sensor fiber, refractive-index resolution of

$$R = \Delta n_a \Delta\lambda_{\min}/\Delta\lambda_{\text{peak}} \approx 1 \times 10^{-4} \tag{6}$$

can be attained by choosing $n_c = 1.45$. Here, the parameter $\Delta n_a = 0.01$ is the difference in the refractive indices of the two analytes, and the peak shift is estimated from Fig. 3(b) to be $\Delta\lambda_{\text{peak}} \approx 10$ nm. The instrumental peak-wavelength resolution is assumed to be $\Delta\lambda_{\min} = 0.1$ nm. In another approach, the transmitted optical power is monitored at a fixed wavelength. For this operation mode, it is useful to introduce a sensitivity parameter [5]

$$S = (\Delta\alpha/\Delta n_a)/\alpha_{1.33}. \tag{7}$$

This parameter is valid for a sensor of length $1/\alpha_{1.33}$, with $\alpha_{1.33}$ denoting the modal loss for the case $n_a = 1.33$. Figure 4 shows the sensitivity S as obtained from the data of Fig. 3(b). By using the data of Fig. 3(a), we confirm that these sensitivity curves do not depend on the value of the parameter s which can also in this operation mode be used to exclusively control the loss. If one assumes that a 1% change in the transmitted power can reliably be measured [5], refractive-index changes on the order of 10^{-4} (for $S \approx 80$) could be detected with this configuration.

4. Summary and discussion

We have proposed a novel surface-plasmon-resonance sensor design based on coating a three-hole MOF with a dielectric layer on top of which a gold layer is deposited. The presented

#93743 - $15.00 USD Received 11 Mar 2008; revised 23 Apr 2008; accepted 16 May 2008; published 9 Jun 2008

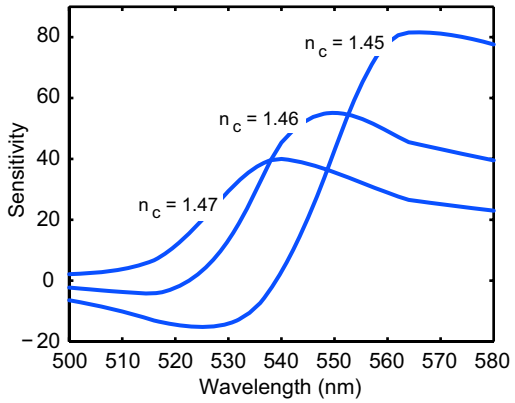

Fig. 4. Sensitivity parameter for the fibers of Fig. 3(b).

design has the following advantages. First, the holes of the three-hole MOF can be tens of micrometers in diameter, which should facilitate the fabrication of the layered sensor structure and the infiltration of the analyte. Second, a single design parameter can be used to tune the loss level of the sensor without affecting the other plasmon-resonance characteristics. Third, the sensor can be made to support a single transverse mode which is essentially Gaussian in shape. Finally, the refractive-index resolution is estimated to be 1×10^{-4} which is comparable to the figure given in Ref. [5].

We remark that the first fabrication step, i.e., the production of the auxiliary dielectric layer, could alternatively be done by using the usual stack-and-draw technique. For instance, in Ref. [16], this technique was used with an appropriate preform to produce annular up-doped layers (within a hexagonal lattice). We believe that this approach could also be used with three-hole MOFs to produce down-doped, low-index layers on the hole surfaces. Yet another approach would be to use a three-hole MOF with an up-doped core, similar to the one presented in Ref. [11]. This way, one could attain efficient mode confinement for controlling the modal loss without using a separate low-index dielectric layer. In closing, we note that besides gold, also copper was found to exhibit a clearly distinguishable plasmon resonance in the course of our numerical investigations.

Acknowledgments

This work has been funded by the Academy of Finland (project nos. 210777 and 124165). Part of the work was conducted within the COST 299 – Fides. Additionally, M. Hautakorpi acknowledges the Finnish Cultural Foundation for funding in the early stages of this research.

#93743 - $15.00 USD Received 11 Mar 2008; revised 23 Apr 2008; accepted 16 May 2008; published 9 Jun 2008